

A novel PSO-based algorithm for structural damage detection using Bayesian multi-sample objective function

Ze-peng Chen^{1,2a} and Ling Yu^{*1,2,3}

¹School of Mechanics and Construction Engineering, Jinan University, Guangzhou 510632, China

²MOE Key Lab of Disaster Forecast and Control in Engineering, Jinan University, Guangzhou 510632, China

³College of Civil Engineering and Architecture, China Three Gorges University, Yichang 443002, China

(Received October 26, 2016, Revised March 24, 2017, Accepted May 12, 2017)

Abstract. Significant improvements to methodologies on structural damage detection (SDD) have emerged in recent years. However, many methods are related to inversion computation which is prone to be ill-posed or ill-conditioning, leading to low-computing efficiency or inaccurate results. To explore a more accurate solution with satisfactory efficiency, a PSO-INM algorithm, combining particle swarm optimization (PSO) algorithm and an improved Nelder-Mead method (INM), is proposed to solve multi-sample objective function defined based on Bayesian inference in this study. The PSO-based algorithm, as a heuristic algorithm, is reliable to explore solution to SDD problem converted into a constrained optimization problem in mathematics. And the multi-sample objective function provides a stable pattern under different level of noise. Advantages of multi-sample objective function and its superior over traditional objective function are studied. Numerical simulation results of a two-storey frame structure show that the proposed method is sensitive to multi-damage cases. For further confirming accuracy of the proposed method, the ASCE 4-storey benchmark frame structure subjected to single and multiple damage cases is employed. Different kinds of modal identification methods are utilized to extract structural modal data from noise-contaminating acceleration responses. The illustrated results show that the proposed method is efficient to exact locations and extents of induced damages in structures.

Keywords: structural damage detection; PSO-INM; multi-sample objective function; benchmark model

1. Introduction

As one of major parts of structural health monitoring, structural damage detection (SDD) methodologies have been developed to monitoring the possible damages emerging in structures. Both static and dynamic responses of structures are basic data of assessment of structural safety. The losses of structural stiffness is a commonly used index to quantify damage extent of structures. In the last two decades, SDD have been widely investigated and achieved great successes. The basic idea of SDD is to find the changed structural properties from measured responses before and after severe events such as hurricane, earthquake, deterioration due to aging and so on (Farrar and Worden 2007, Li and Chen 2013). For a better description of structural damage, a class of models are generally defined based on assumed relationships between input and output variables of structural system (Teughels and De Roeck 2005). Such model-based techniques, named model updating, realize SDD process by transferring it into minimizing difference between measured and theoretical output data of structures. Generally, there are two major kind of output data, time domain data and frequency domain data (Yu and Lin 2015). Time domain data include displacement, acceleration, strain

and so on. Damage indices are defined in time domain method and most of them are based on statistical moments (Chen and Xu 2007, Yu and Zhu 2015) of structural responses. As precise knowledge of input excitation is required (Simoen *et al.* 2015), time domain data are rarely used directly for modal updating. On the contrary, frequency domain parameters are natural characters of structures and they are invariant in spite of what kind of excitation (i.e., impulse excitation, random excitation or vehicle load) are applied; therefore, the frequency domain data are more are employed popularly in the field of model updating. Frequency domain data contain frequency, mode shape, modal flexibility (Pandey and Biswas 1994), modal curvature (Pandey *et al.* 1991), and modal strain energy (Shi *et al.* 2000). They are all sensitive damage index. In this study, in order to detect damage in multiple locations a new SDD method is proposed via defining a multi-sample objective function with frequencies and mode shapes and a hybrid particle swarm optimization (PSO) algorithm is applied to solve the SDD problem of a 2 storey frame and ASCE 4-storey benchmark frame structure.

SDD is a typical inverse problem (Friswell 2008). Decomposition method such as singular value decomposition (SVD), QR factorization or Cholesky factorization, and regularization techniques have been developed to solve the SDD problem. The disadvantages of them are that they include inverse computation, which calculate model properties such as mass and stiffness from measurement data on frequencies or mode shapes (Simoen

*Corresponding author, Professor

E-mail: lyu1997@163.com

^aPh.D. Student

et al. 2015). Then being ill-posed or ill-conditioning emerge, leading to an unstable solutions with respect to small changes in the measured data. With the rapidly development of computation technologies, massive of intelligent algorithms, such as genetic algorithm (GA) (Yan *et al.* 2007), ant colony optimization (ACO) (Yu and Xu 2011), artificial fish swarm algorithm (AFSA) (Yu and Li 2014), firefly algorithm (FA) (Pan *et al.* 2016), Artificial Bee Colony algorithm (ABC) (Xu *et al.* 2015) and PSO (Baghmisheh *et al.* 2012, Seyedpoor 2012), become innovative techniques dealing SDD issues. The current status of structures can be estimated by minimizing fitness value of objective function (or cost function, fitness function). The objective function is defined as difference between measured and theoretical output data. Among these techniques, the PSO based algorithm has been confirmed effective due to its good performance in global searching. PSO is simple in concept and does not involve inverse analysis. However, the accuracy of optimization algorithm is affected by its randomness which is the theoretical basis of the algorithm. The randomness of PSO, such as particle initial distribution and random numbers containing in the manipulating equation, ensures the algorithm to search whole feasible space but sometimes makes it fall into wrong solution, which are generally called local optimum. However, some improved strategies have been investigated to deal with such weakness. Baghmisheh *et al.* (2012) adopted a hybrid PSO-NM algorithm for damage assessment based on PSO and Nelder-Mead simplex algorithm (NM). Seyedpoor *et al.* (2012) proposed a two-step algorithm which reduces the dimension of optimal parameters for a more accurate results. Gerist and Maheri (2016) presented a BP-PSO-MS algorithm to improve the accuracy of detecting multiple damage cases.

Another factor affects the accuracy of PSO is uncertainty of model and response data. Due to complex and indeterminate environment around the structure, the output data tends to show significant variation from one test to another. The disturbance of environment is described as noise. Therefore, idealized numerical prediction models are unable to perfectly represent behaviors of the structure. Probabilistic analysis is a common used method for uncertainty quantification (Simoen *et al.* 2015). Probability density functions (PDFs) are always pointed to the uncertain variables and Bayesian method is a classical model for probability analysis. Beck (Beck *et al.* 1999, Ching and Beck 2004, Cheung and Beck 2009) and Yuen (Yuen and Kuok 2001, Yuen *et al.* 2004) have made great contribution to establish a Bayesian statistical framework for SHM. Beck *et al.* (2002) firstly presented a Bayesian statistical framework for system identification and applied the theory to continual on-line SHM using vibration data from structures. However, the appearance of different Bayesian approach such as Bayesian spectral density approach (Katafygiotis and Yuen 2001), Bayesian spectral density approach time domain method (Yuen and Katafygiotis 2001) and Bayesian FFT approach (Yuen and Katafygiotis 2003) have made great developments of Bayesian inference in SHM. Au and Zhang (2012) and Zhang *et al.* (2015) have demonstrated a Fast Bayesian

approach for modal identification both suitable for using ambient vibration data and free vibration data, and the methods are also successfully applied to SHM of Shanghai Tower (Zhang *et al.* 2016). Recently, Au and Zhang (2016, 2016) developed a fundamental two-stage formulation for Bayesian system identification and Jensen *et al.* (2017) have also achieved good implementation of an adaptive meta-model for Bayesian finite element model updating in time domain.

From the previous work, it is seen that most of intelligent algorithms focus on solving a single or multiple objective function based on single data sample, which sometimes leads to an unstable solution. And few researches have tried to maximize the likelihood function in Bayesian inference utilizing intelligent algorithms. To make a combination of Bayesian inference and intelligent algorithm for gaining a more stable solution, a multi-sample objective function is defined based on Bayesian inference and then optimized by a hybrid PSO algorithm in this paper. Numerical simulations on a 2-storey rigid frame structure using frequency and mode shape information show that the proposed method is effective for accurately identifying the location and extent of multiple structural damages. Further, the ASCE 4-storey benchmark frame structure is adapted to assess the performance of the proposed method based on the acceleration responses of structures. Complex pursuit (CP) algorithm and covariance-driven stochastic subspace identification (SSI-COV) are both used to extract modal data for SDD under different damage cases. The illustrated results show that the proposed method is also a reliable SDD tool for the ASCE benchmark frame structure.

2. Theoretical background

2.1 SDD formulation

SDD problem has been deeply investigated in the field of SHM. When a finite element model is available, the damage is considered as reduction of stiffness and mass of structures. Assuming the change in mass can be ignored comparing with the stiffness (Begambre and Laier 2009). Then, the linear relationship between structural stiffness matrix and element stiffness matrix can be adopted as follows

$$\mathbf{K}(\boldsymbol{\theta}) = \sum_{i=1}^{N_e} (1 - \theta_i) \mathbf{K}_i \quad (1)$$

in which $\boldsymbol{\theta}$ is a vector of damage factor with same length of N_e element numbers and ranges from 0 to 1. $\theta_i=0$ means undamaged state. \mathbf{K} and \mathbf{K}_i represent structural global stiffness matrix and i -th element stiffness matrix respectively. The dynamic behavior of structural finite element model (FEM) under excitation force $\mathbf{F}(t)$ can be written as

$$\mathbf{M}\ddot{\mathbf{u}} + \mathbf{C}(\boldsymbol{\theta})\dot{\mathbf{u}} + \mathbf{K}(\boldsymbol{\theta})\mathbf{u} = \mathbf{F}(t) \quad (2)$$

where \mathbf{M} , $\mathbf{C}(\boldsymbol{\theta})$ are structural mass and damping matrix, respectively. $\ddot{\mathbf{u}}$, $\dot{\mathbf{u}}$, \mathbf{u} are corresponding acceleration,

velocity and displacement vector respectively. The m -th undamped frequency ω_m and mode shape $\boldsymbol{\varphi}_m$ are extracted from the characteristic Eq. (3) derived from Eq. (2)

$$[\mathbf{M} - \omega_m^2 \mathbf{K}(\boldsymbol{\theta})] \boldsymbol{\varphi}_m = \mathbf{0} \quad (3)$$

2.2 PSO-INM algorithm

PSO is a population-based, self-adaptive search technique. The possible solution of the optimization problem is considered as a point, called ‘‘particle’’, locating in the multi-dimension space. The PSO starts with a random population of particles (feasible solution) among the search space and then determines the global best solutions by adjusting the trajectory of each particle towards its own best location and the best particle of the entire swarm. The PSO method is a simple, efficient and fast convergence algorithm; therefore, it is popular in solving optimization problem. However, more detail of how PSO implements in optimization can be found in (Chen and Yu 2015).

The PSO-INM is a method for solving the model updating problem described above. It is hybrid algorithm combining PSO and improved Nelder-Mead method (INM). The basic idea of PSO-INM is to search the local area around optimum solution $\boldsymbol{\theta}^*$ found by PSO using INM. The INM’s perfect local searching ability helps to increase the $\boldsymbol{\theta}^*$ ’s precision. More details of PSO-INM algorithm is referred in (Chen and Yu 2015).

Traditional objective function is usually based on modal data, i.e., the relative percentage errors (RPE) of frequencies and modal assurance criterion (MAC) of the mode shapes in the following form

$$\begin{aligned} \text{Obj1} : \boldsymbol{\theta}^* &= \arg \min_{\boldsymbol{\theta}} F(\boldsymbol{\theta}) = \\ & \arg \min_{\boldsymbol{\theta}} \sum_{m=1}^{N_m} \left[1 - \text{MAC}(\boldsymbol{\varphi}_m^c, \boldsymbol{\varphi}_m^a) + \text{RPE}(\omega_m^c, \omega_m^a) \right] \end{aligned} \quad (4)$$

where

$$\text{MAC}(\boldsymbol{\varphi}_m^c, \boldsymbol{\varphi}_m^a) = \frac{|\boldsymbol{\varphi}_m^{cT} \boldsymbol{\varphi}_m^a|^2}{|\boldsymbol{\varphi}_m^{cT} \boldsymbol{\varphi}_m^c| |\boldsymbol{\varphi}_m^{aT} \boldsymbol{\varphi}_m^a|}, (m = 1, 2, \dots, N_m)$$

represents MAC between the m -th calculated mode shape $\boldsymbol{\varphi}_m^c$ and the m -th actual mode shape $\boldsymbol{\varphi}_m^a$ within the first N_m modal data. $\text{RPE}(\omega_m^c, \omega_m^a) = \left| \frac{\omega_m^a - \omega_m^c}{\omega_m^a} \right| \times 100\%$ is the

RPE between the m -th calculated frequency ω_m^c and the actual frequency ω_m^a . When the calculated modal data are equal to the actual ones, the objective function gets its minimum value of zero. The corresponding solution $\boldsymbol{\theta}^*$ is regarded as the structural state.

For real structures, measured data are contaminated by noise, which is considered as a zero-mean stationary Gaussian white-noise process in numerical simulation. The formulation of noise-adding can be described as follows

$$\mathbf{D}_{\text{noise}} = \mathbf{D} + \varepsilon \boldsymbol{\Psi} \mathbf{R} \quad (5)$$

where $\mathbf{D}_{\text{noise}}$, \mathbf{D} are measured data with and without noise, respectively. ε is noise level ranging from 0 to 1 and \mathbf{R} is

a vector with random values obeying the distribution $N(0, 1)$. $\boldsymbol{\Psi}$ is value of frequency for frequency data or it is calculated by Eq. (6) when mode shapes with N_n nodes are considered.

$$\boldsymbol{\Psi} = \sqrt{\frac{1}{N_n N_m} \sum_{n=1}^{N_n} \sum_{m=1}^{N_m} \varphi_{nm}^2} \quad (6)$$

2.3 Bayesian theory

To remove the noise negative effect from the optimal process, the idea of Bayesian theory is referred to form a more effective objective function and help to distinguish spurious damaged elements out of the solution.

The probabilistic SHM framework based on Bayesian theory was firstly presented by Beck *et al.* (2002) and applied for a simulating on-line monitoring. The significant basis of Bayesian theory is the conditional probability, which assumed the prior knowledge attributed to a certain events or hypothesis. The Bayesian interpretation provide a rigorous process for uncertainty quantification. Bayesian theory used in the SHM field to express the updated probabilities of model parameter $\boldsymbol{\theta}$ has the mathematical form as

$$p(\boldsymbol{\theta} | \mathbf{D}) = c p(\mathbf{D} | \boldsymbol{\theta}) p(\boldsymbol{\theta}) \quad (7)$$

where $p(\boldsymbol{\theta} | \mathbf{D})$ is probability density function (PDF) of model parameters given the modal data \mathbf{D} and the assumed FEM, and $p(\mathbf{D} | \boldsymbol{\theta})$ is PDF of modal data given the model parameter $\boldsymbol{\theta}$, which is more widely known as likelihood function. $p(\boldsymbol{\theta})$ is prior PDF of model parameters $\boldsymbol{\theta}$ based on engineering and modeling judgments. c is a constant which ensures the integral of $p(\boldsymbol{\theta} | \mathbf{D})$ to be one. Taking $\mathbf{D} = [\mathbf{D}_1, \mathbf{D}_2, \dots, \mathbf{D}_{N_s}]$ as observing modal data with N_s samples, $\mathbf{D}_s = [\omega_{1,s}, \omega_{2,s}, \dots, \omega_{m,s}, \boldsymbol{\varphi}_{1,s}, \boldsymbol{\varphi}_{2,s}, \dots, \boldsymbol{\varphi}_{m,s}]$ represents the s -th sample of frequencies and mode shapes. Then the likelihood function becomes

$$p(\mathbf{D} | \boldsymbol{\theta}) = \prod_{s=1}^{N_s} p(\mathbf{D}_s | \boldsymbol{\theta}) = \prod_{s=1}^{N_s} \left(\prod_{m=1}^{N_m} p(\omega_{m,s} | \boldsymbol{\theta}) p(\boldsymbol{\varphi}_{m,s} | \boldsymbol{\theta}) \right) \quad (8)$$

It is assumed that test and modal data are independent. The principle of maximum entropy is used as a justification to choose a Gaussian distribution for $\omega_{m,s}$ and $\boldsymbol{\varphi}_{m,s}$. Then the resulting PDFs of $\omega_{m,s}$ and $\boldsymbol{\varphi}_{m,s}$ are calculated as follow respectively

$$p(\omega_{m,s} | \boldsymbol{\theta}) = c_1 \exp \left[-\frac{(\omega_{m,s} - \omega_m^a)^2}{2\varepsilon_m^2} \right] \quad (9)$$

$$p(\boldsymbol{\varphi}_{m,s} | \boldsymbol{\theta}) = c_2 \exp \left[-\frac{(\boldsymbol{\varphi}_{m,s} - \boldsymbol{\varphi}_m^a)^T (\boldsymbol{\varphi}_{m,s} - \boldsymbol{\varphi}_m^a)}{2\delta_m^2} \right] \quad (10)$$

where, ε_m^2 and δ_m^2 are the variance of the m -th frequency and the diagonal element of covariance matrix C_m , respectively. The covariance matrix C_m of the m -th mode shape is simplified as $C_m = \delta_m^2 \mathbf{I}_{N_m \times N_m}$. The sample variances are used to approximate the variances of Gaussian

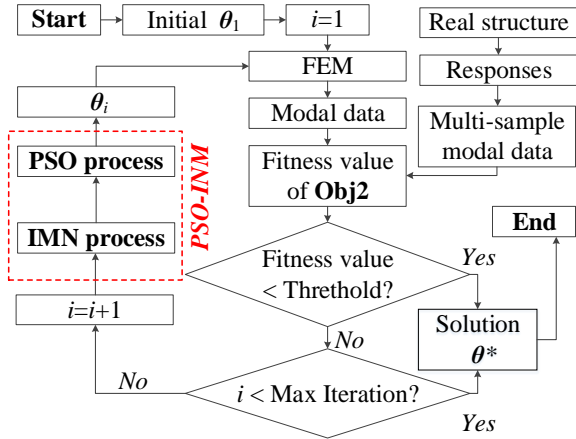


Fig. 1 Flowchart of proposed method

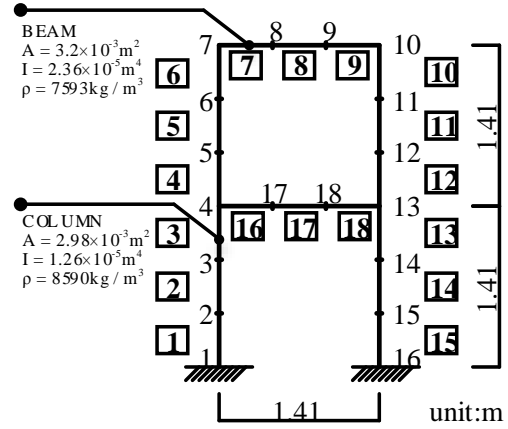


Fig. 2 Finite element model of two-storey rigid frame structure

distribution ε_m^2 and δ_m^2 which can be calculated as follows

$$\varepsilon_m^2 = \frac{1}{N_s - 1} \sum_{s=1}^{N_s} (\omega_{m,s} - \bar{\omega}_m)^2, \quad (11)$$

$$\delta_m^2 = \frac{1}{N_s - 1} \sum_{s=1}^{N_s} \|\varphi_{m,s} - \bar{\varphi}_m\|^2$$

The prior distribution of model parameters θ is assumed to be uniform distribution, which means that its PDF has the form:

$$p(\theta) = c_3 \quad (12)$$

where c_3 is a constant.

Substituting Eqs. (9) and (10) into Eq. (8), then combining Eqs. (8) and (12) yields the final form of $p(\theta|\mathbf{D})$ as shown in Eq. (13)

$$p(\theta|\mathbf{D}) = c \exp \left[- \sum_{s=1}^{N_s} \sum_{m=1}^{N_m} \left[\frac{(\omega_{m,s} - \omega_m^a)^2}{2\varepsilon_m^2} + \frac{(\varphi_{m,s} - \varphi_m^a)^T (\varphi_{m,s} - \varphi_m^a)}{2\delta_m^2} \right] \right] \quad (13)$$

The goal of Bayesian-based probabilistic analysis is to maximize the probability of $p(\theta|\mathbf{D})$ based on the known test data and then ascertain the most likely damaged elements.

Based on the Bayesian analysis process, a multi-sample objective function is proposed to maximize the likelihood probability function $p(\theta|\mathbf{D})$, which can be converted into a minimization optimization problem written as Eq. (14). The aim of the multi-sample objective function is to make full use of the data sets but not use the average value only. The advantages of multi-sample objective function will be explored in the next section. The flow chart of the proposed method is shown as Fig. 1.

$$Obj2: \theta^* = \arg \min_{\theta} J(\theta) = \arg \min_{\theta} \left\{ \sum_{s=1}^{N_s} \sum_{m=1}^{N_m} \left[\frac{(\omega_{m,s} - \omega_m^a)^2}{2\varepsilon_m^2} + \frac{(\varphi_{m,s} - \varphi_m^a)^T (\varphi_{m,s} - \varphi_m^a)}{2\delta_m^2} \right] \right\} \quad (14)$$

Table 1 Damage cases

Cases	Description
1	5% @ 17
2	10% @ 17
3	20% @ 17
4	40% @ 17
5	20% @ 8, 20% @ 17
6	10% @ 8, 20% @ 17
7	15% @ 5, 20% @ 8, 30% @ 17
8	25% @ 5, 25% @ 8, 25% @ 11, 25% @ 17

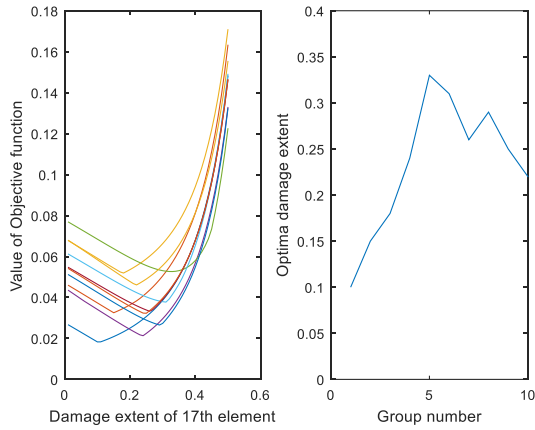
3. Numerical simulations

3.1 Two-storey rigid frame structure

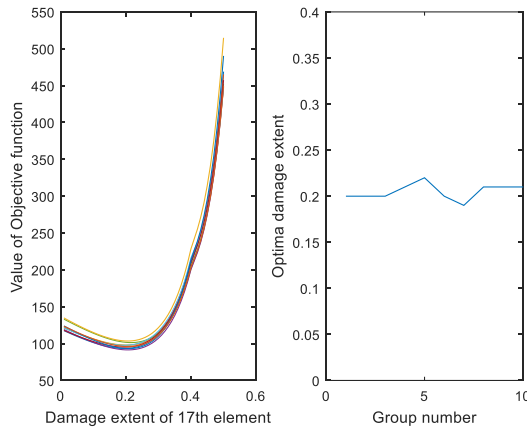
A two-storey rigid frame structure is adopted to assess the performance of the proposed method. The diagram of structure, physical dimensions and material properties are shown in Fig. 2. The elastic modulus of both beam and column are equal to 2.1×10^{11} N/m². The numbers in the box represent finite element number, while others denote measured node number.

The frame structure is modeled by 18 two-dimension beam elements with equal length. Several damage scenarios are simulated by setting different value in the damage coefficient vector θ . Single damage is introduced in the 17th element ranging from 5% to 40%. Different combination of elements with different damage extents are simulated to identify the multi-damage cases. The damage element location and extent are listed in Table 1. The symbol 5% @ 17 in Table 1 indicates that the stiffness of the 17th element is decreased by 5%, similar meaning for other cases.

The first five modal frequencies and mode shapes are adopted, meaning $N_m=5$. The number of modal parameters is determined based on reference (Yu and Li 2014). The mode shape is measured along the vertical direction of components; accordingly, the vertical direction of beam and the horizontal direction of column are available. Noises are contaminated in frequencies and mode shapes based on Eq. (5), and the noise level are 3% and 5% respectively.



(a) for traditional objective function



(b) for multi-sample objective function

Fig. 3 Comparison on results due to objective functions

3.2 Comparison on different objective functions

Case 3 is used to investigate effects of noise on objective functions. Assuming the damage location is determinate, the objective function becomes a single variable function with respect to damage extent at 17th element. Noises are added up to the original modal data in Case 3 to generate 100 samples. Dividing these data into 10 groups with equal sample size of 10. The fitness value of objective functions, based on Eqs. (4) and (14), are calculated using different group of data. The average values of each group data are adopted for traditional objective functions. Fig. 3(a) is the result due to traditional objective function while Fig. 3(b) is that due to the proposed one. The left plot of each figure describes the pattern of objective function with respect to damage extent at 17th element and the right one demonstrates the optimal damage extent corresponding to the minimal objective function value for every group. By comparison, the optimal damage extent of multi-sample objective function in Fig. 3(b), which varied within a small range of real damage extent 20%, is more stable than the traditional one in Fig. 3(a). Under the effect of noise, the optimal solution of traditional objective function deviated from the actual one, leading to an error identification even if the algorithm has a great optimal ability. On the contrary, the optimal solution of multi-sample objective function is stable for different group of

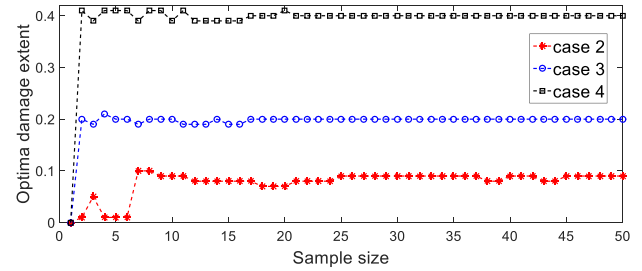


Fig. 4 Optimal damage extent with respect to sample size

data. The advantages of multi-sample objective function make it more suitable for optimal algorithm and help to improve the accuracy of SDD results.

3.3 Sample size for objective functions

Because multiple samples are necessary for the proposed objective function, the sample size is an important parameter to be assessed. A small sample size cannot guarantee the stability of objective functions while the large one would waste the computing resource. The sample size is assessed by single damage cases for convenience. The optimal damage extent in Cases 2 to 4 with respect to sample size are shown in Fig. 4. It can be found from Fig. 4 that the optimal damage extents become gradually stable with increasing sample size. When the sample size is higher than 10, the optimal damage extents of all the single cases remain around the real one. Therefore, the sample size is set to be 10 and extended for other multi-damage cases.

3.4 SDD results

As shown in Table 1, there are 4 single damage cases with damage at 17th element. All the SDD results using the PSO-INM are shown in Fig. 5. Optimal solutions were obtained from fifty independent distributed runs for each case. The sample size is 10 and the average values are adopted for traditional objective function. The symbol “Obj2” and “Obj1” in Fig. 5(a) are corresponded to results of the multi-sample objective function and the traditional objective function respectively.

Fig. 5 shows that the damage factor at 17th element is obviously greater than that at other elements. It means that the damage location can be assessed well. Some error identified elements also exist mostly around the 17th element, such as 16th and 18th elements. The identified result for Case 2 is the worst one where elements around the 3rd element keep a quite high value of damage factor. The identified damage at 18th element in Case 1, as shown in Fig. 5(a), is smaller than that in Obj1, which means that the proposed objective function outperform the traditional one in the case of small damage, i.e., 5% stiffness reduced in element. After the damage gradually increases, both objective functions show their advantage in assessing the damage location and extent because effects of stiffness change in modal data predominate the noise.

All the SDD results for multi-damage cases, i.e., Cases 5 to 8 as listed in Table 1, are shown in Fig. 6. For all the multi-damage cases, the multi-sample objective function

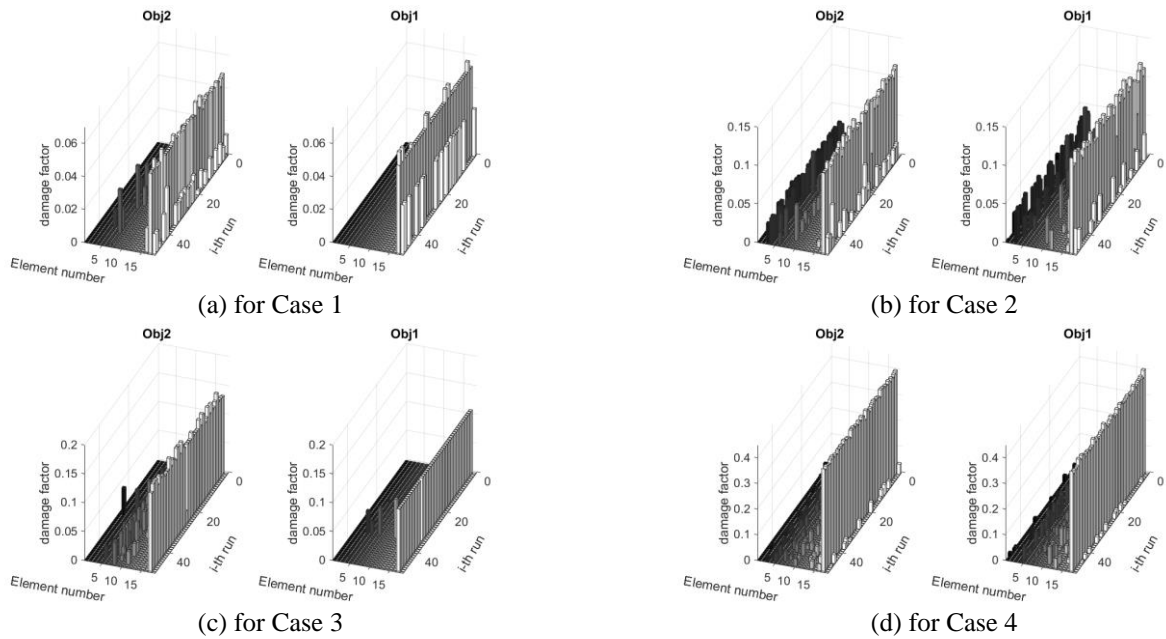


Fig. 5 SDD results for all single cases

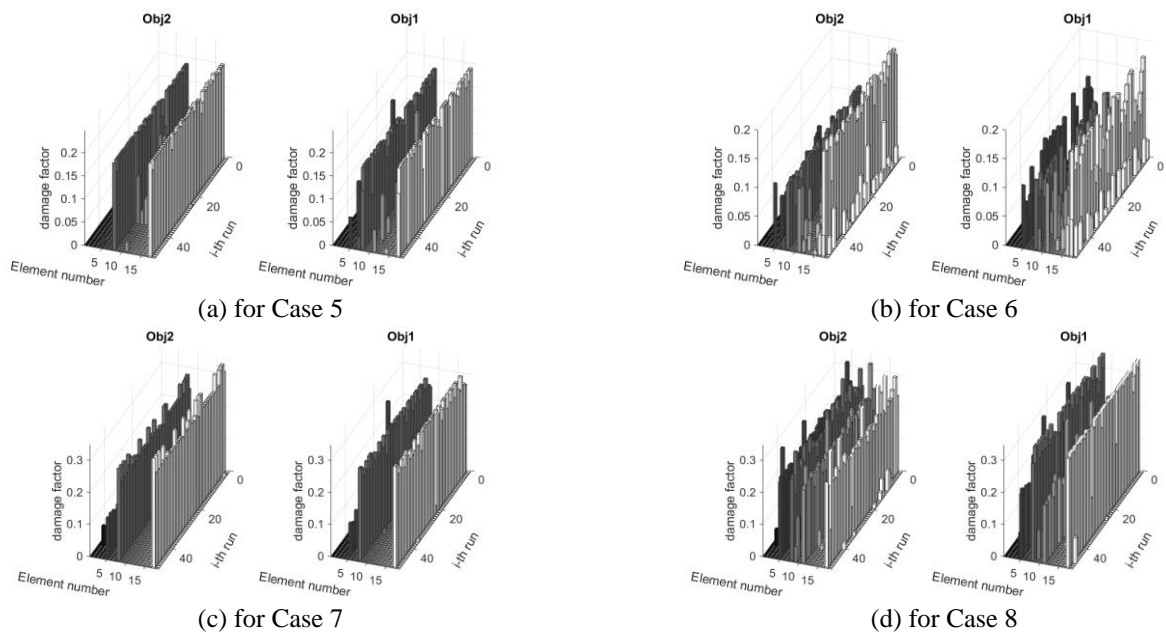


Fig. 6 SDD results for multi-damage cases

shows its greater capability of assessing damage than the traditional one. The conclusion can be confirmed strongly from Case 6, which includes two damages in 8th and 17th elements respectively. As shown in Fig. 6(b), two evident high bars of Obj2 can be recognized at 8th and 17th elements, which helps to locate damage and their extent. On the contrary, there are at least four stable bars in case 6 due to Obj1 as in Fig. 6(b), which means two health elements are misjudged as damaged elements using traditional objective function. However, the results for Case 8 in Fig. 6(d) provide further evidence that the multi-sample objective function is more accurate in quantifying the damage extent than that due to the traditional objective function. There are four damaged elements with equal

stiffness reduction in Case 8. The results of Obj2 in Fig. 6(d) show the characteristic of equal damage extent in 5th, 8th, 11th and 17th elements evidently, while that of Obj1 show damage factors at 5th and 11th elements are obviously lower than that at 8th and 17th elements.

The illustrated SDD results for both single and multiple damage cases indicate that the proposed method, using multi-sample objective function for optimization, can not only locate structural damage effectively but also quantify damage extent with an improved higher accuracy.

For a more specific understanding of the identified results, average value and it plus and minus standard deviation are plotted in Fig. 7. That short lines upon and below bars represent average value plus and minus standard

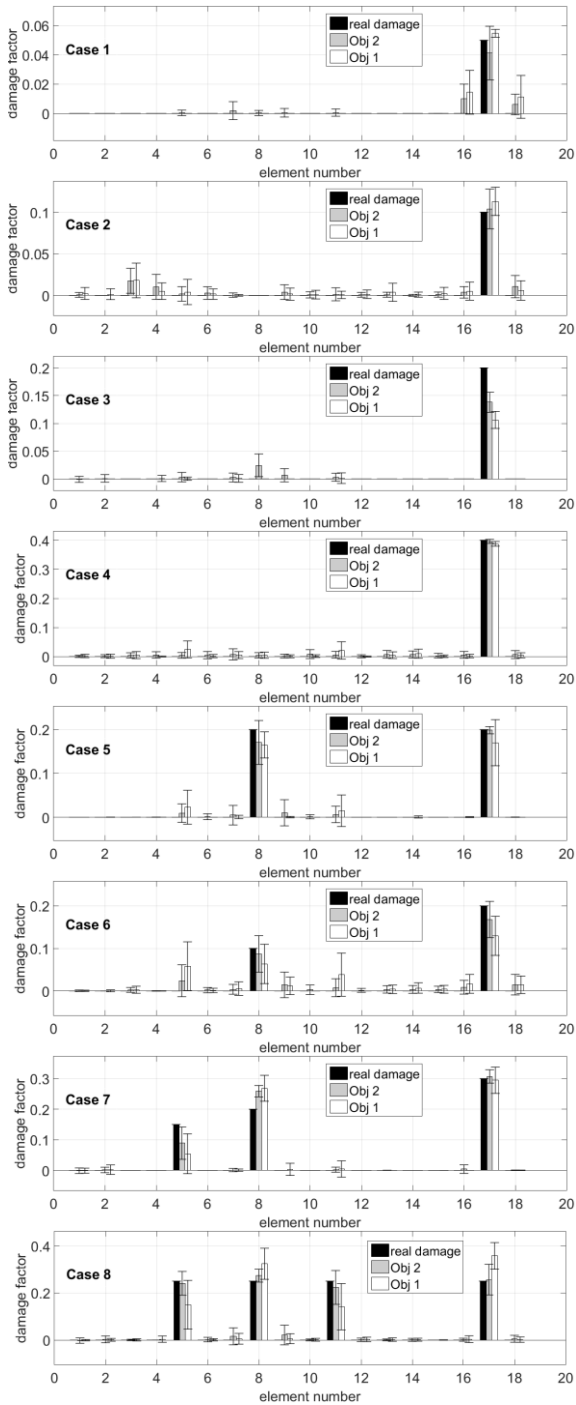


Fig. 7 Average value and average plus and minus standard deviation of each cases

deviation respectively. Base on average values, same conclusions can be also drawn that the multi-sample objective function outperform the traditional objective function in both locating multi-damage and quantifying damage extent. The proposed method can give a more reliable identification results than traditional ones.

4. Benchmark model verification

In this part, a Benchmark model of four-storey, two-bay

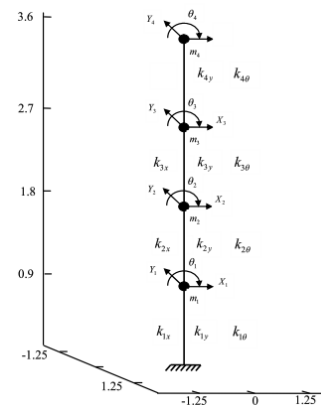


Fig. 8 12-DOF model

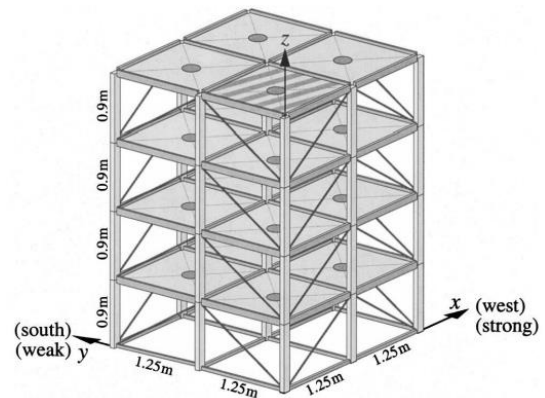


Fig. 9 120-DOF model

by two-bay steel-frame quarter-scale structure proposed by IASC-ASCE Structural Health Monitoring Task Groups is further utilized to verify the proposed method. The Benchmark model was created for side-by-side comparison among different monitoring methods numerically and experimentally. The properties of structural members can be found in detail in paper (Johnson *et al.* 2004). There are 45 nodes of the structure model and 9 of them are totally constrained on the basement. The columns and floor beams are simulated as Euler-Bernoulli beams. Two kinds of reduced finite element models are developed to simplify the model calculation. The first one is a 12 degree of freedom (DOF) model (as seen in Fig. 8) which considers each floor as a lump mass with 3 DOF, two horizontal translation and one rotation. The Second one is a 120-DOF model (as seen in Fig. 9), assuming nodes at the same floor have the same horizontal translation and in-plane rotation, is simulated by Euler-Bernoulli beams with 6 DOF at each nodes.

The symmetric 12-DOF model is applied for verification in this paper. Four damage cases and the intact state are studied. The damage cases are defined as: 1) remove all braces in the first storey; 2) remove all braces in the first and the third stories; 3) remove only one brace in the first storey which located in the plane $y=0$ with x coordinate ranging from 1.25 to 2.5; 4) remove one brace respectively in the first storey and in the third floor, which located in the plane $y=0$ with x coordinate ranging from 1.25 to 2.5. The SDD is processed by detecting the stiffness loss of y -direction.

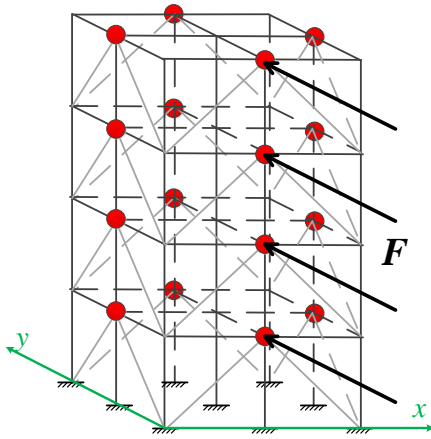


Fig. 10 Loading and measured diagram (point “●” means acceleration measured point and arrow means excitation applied point)

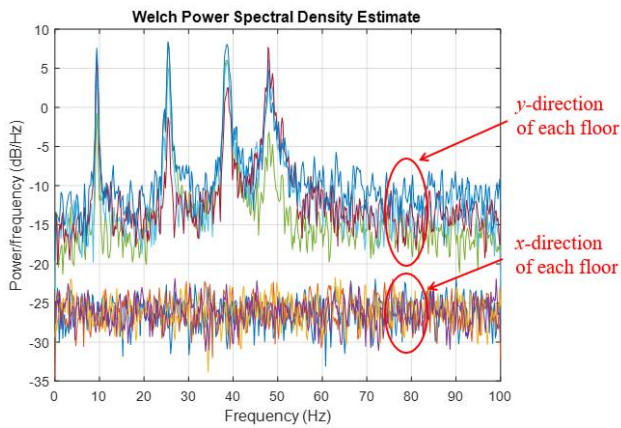


Fig. 11 PSD of signals at different floor along x and y direction

The acceleration signals are measured at the node as points shown in Fig. 10 and the measured freedoms are all along the coordinate direction. Excitations applied at different nodes are the independent Gaussian white noise with 150N intense. The sample frequency is 200Hz and a 20s time history signal is recorded. The loading and measured diagram are shown detail in Fig. 10. An integration method termed fast Nigham-Jennings is used to calculate the time history of acceleration responses. Damping ratio is assumed as 0.01 in each mode. Noise contaminated in the acceleration signals is considered as 10%.

As the structure is symmetric and excitations are loaded at the symmetry axis, responses of nodes at $x=0$ and $x=2.5$ m at the same floor are identical. The y -direction excitation loading at the symmetry axis will only activate responses and mode shape along y -direction, which are coincident with the PSD results as shown in Fig. 11. Only four peaks are observable for the measured calculation responses along y -direction, which means that the first four vibration modes along y -direction are activated under excitation adapted in this paper.

4.1 Modal parameters extraction

Table 2 Modal data extraction in undamaged case using CP

Mode	Frequency/Hz			MAC			
	True	Estimate	Error	1	2	3	4
1	9.29	9.38	0.91%	0.9983	0.0587	0.0130	0.0159
2	25.27	25.39	0.47%	0.0174	0.9948	0.0598	0.0033
3	38.26	38.67	1.07%	0.0075	0.0445	0.9984	0.0186
4	47.75	47.85	0.21%	0.0123	0.0042	0.0185	0.9995

Table 3 Modal data extraction in undamaged case using SSI

Mode	Frequency/Hz			MAC			
	True	Estimate	Error	1	2	3	4
1	9.29	9.42	1.38%	0.9983	0.0200	0.0067	0.0125
2	25.27	25.51	0.93%	0.0265	0.9963	0.0445	0.0034
3	38.26	38.68	1.11%	0.0103	0.0267	0.9989	0.0178
4	47.75	48.09	0.70%	0.0056	0.0028	0.0233	0.9998

Once the accelerations are measured among different nodes, methods should be used to extract modal parameters such as natural frequencies and mode shapes. A traditional modal extraction method termed covariance-driven stochastic subspace identification (SSI-COV) and a novel unsupervised learning algorithm Complexity Pursuit (CP) algorithm is applied to gather modal data in this study.

Here, the SSI-COV is an output-only modal analysis technique which is widely used to extract modal data from ambient vibration responses (Peeters and Roeck 2001). The main procedure of SSI-COV contains constructing the Toeplitz matrix $T_{1|i}$ and $T_{2|i+1}$ based on output covariance R_i , decomposing $T_{1|i}$ and $T_{2|i+1}$ based on singular value decomposition (SVD) technique and evaluating state transition matrix A and output matrix C . Frequencies and mode shapes can be recovered from A and C .

While the CP algorithm was first proposed by Stone (2001) to solve blind source separation (BSS) problems and was applied to modal identification recently (Yang and Nagarajaiah 2013, Yang *et al.* 2015). The method assumes that temporal predictability of a mixed signal is less than any component signals contributing to it. Consequently, the decoupled modal responses can be recovered from structural responses for obtaining modal parameters.

Both SSI-COV and CP are applied because they represent two different ways to extract modal parameters: one is covariance-driven technique, the other is BSS-based. Modal data extracted from both techniques are imported to SDD process to verify availability of the proposed method.

4.2 Undamaged case study

A comparison on true modal data and estimated ones are listed in Tables 2 and 3. It can be seen from Tables 2 and 3 that the highest error of both method is smaller than 1.5% from which we can see them the same.

The MAC between true and estimated mode shapes are closed to one at all the diagonal elements but approach to zero at all the non-diagonal elements. They indicate that both SSI-COV and CP are available to provide accurate modal data for SDD.

Table 4 Frequencies (Hz) in different cases

Mode	Case 1		Case 2		Case 3		Case 4	
	CP	SSI	CP	SSI	CP	SSI	CP	SSI
1	6.250	6.2486	5.859	5.8393	8.887	8.8615	8.887	8.8650
2	21.480	21.5440	14.840	14.8761	24.510	24.5651	24.510	24.5587
3	37.400	37.4776	36.130	36.1185	38.090	38.2299	38.090	38.2253
4	47.850	47.8961	41.410	41.3033	47.850	48.0391	47.850	48.0375

4.3 Identification of damaged storey stiffness along y -direction

Originally, more than one modal data sample is required for the proposed method in this paper. It is assumed that the modal frequencies vary within $\pm 3\%$ of its real value and mode shapes vary within $\pm 3\%$ of its entries.

Natural frequencies estimated by different modal identification techniques are shown in Table 4. It can be found that frequencies in Cases 3 and 4 are identical. The reason is that the brace removed from the structure is along x -direction both for Cases 3 and 4, resulting few stiffness loss of y -direction. So, in the following discussion, results of Case 4 are not involved.

As shown in Table 5, SDD results, identified by the proposed method for each case, are summarized. The term "damage" is the average value of fifty independent calculation runs. The standard deviation (STD) is also estimated to describe the stability of SDD results. The RPE values of identified damage extent for Cases 1 and 2 are both below 1% while that for Case 3 is a little bit higher. As a suitable finite element model (FEM) is always necessary to quantify damage extent, biases between the modal data estimated by modal identification techniques and by system matrix from FEM are unavoidable, but they are quite small comparing to the changes of modal data from stiffness loss in case of increasing damage extent. The damage extent of Case 3 is the smallest; therefore, the identified results for Cases 1 and 2 would be more accurate than that for Case 3. However, the RPE of Case 3 at 1st floor is close to 10%, meaning a reliable precision for engineering program. On the other hand, although the damage extent quantification for Case 3 is less accurate, damage locations are accurately determined. The moderately overestimation of damage extent will also help to raise the alarm before serious damage emerge. The values of STD as shown in Table 5 also indicate that SDD results of the proposed method are stable under different calculation runs.

It can be also seen from Table 5 that the identified results using modal data extracted by the two methods show a little bit difference. As both methods are based on infinite time series, impossible for practical engineering project on which finite responses time series are available, errors emerge when infinite responses time series are replace by finite ones. This kind of errors are different from different methods and verification can be found in Table 4 that modal frequencies are a little bit different. The error described above would finally lead to differences in Table 5, but we can see them the same as biases between the two methods are all below 0.01.

Table 5 SDD results based on SSI and CP

Case		1 st floor		2 nd floor		3 rd floor		4 th floor	
		Damage	STD	Damage	STD	Damage	STD	Damage	STD
1	Real	0.7103	-	0	-	0	-	0	-
	SSI	0.7089	1.57e-05	-0.0005	3.19e-03	0.0000	5.03e-12	0.0000	2.09e-11
	CP	0.7091	1.19e-05	0.0000	1.64e-18	0.0000	1.18e-11	0.0000	1.38e-11
2	Real	0.7103	-	0	-	0.7103	-	0	-
	SSI	0.7072	1.59e-04	-0.0002	8.03e-04	0.7122	2.48e-04	0.0000	1.14e-04
	CP	0.7036	4.78e-04	0.0001	4.03e-04	0.7152	2.13e-04	0.0000	2.59e-11
3	Real	0.1776	-	0	-	0	-	0	-
	SSI	0.2006	1.18e-05	0.0000	5.22e-26	0.0000	1.67e-11	0.0000	7.48e-12
	CP	0.1957	2.95e-03	0.0077	9.36e-03	0.0004	1.32e-03	0.0059	7.49e-03

Consequently, SDD results on the ASCE 4-storey benchmark frame structure indicates that the proposed method is also applicative while modal data are extracted from different kinds of modal identification techniques and provides a more accuracy solution with great stability.

5. Conclusions

This study makes a trail of combining PSO-based algorithm with Bayesian inference and proposes a method that applies PSO-improved Nelder-Mead method (PSO-INM) to solve optimal problem on Bayesian multi-sample objective function of structural damage detection (SDD). Comparative studies between the proposed multi-sample objective function and the traditional one have been conducted in this paper, which indicate advantages of the multi-sample objective function. SDD numerical simulations on a two-storey rigid frame structure show that the proposed method can not only locate the structural damages effectively but also quantify the damage extents with an improved higher accuracy. The SDD results on the ASCE 4-storey benchmark frame structure further show availability of the proposed method for SDD program whose modal data are extracted from structural acceleration responses. Conclusions can be summarized detail as follows:

1) The proposed SDD method avoid excessively bias of minimum point of objective function which provide more stable identified results under difference independent runs. It helps to improve the accuracy of PSO-based algorithm because the optimum of multi-sample objective function is closer to the actual damage cases. The adverse effect of noise can be greatly reduced if the multi-sample objective function is applied.

2) The proposed method provides a satisfactory precision and stable identification for such SDD engineering programs whose modal parameters are extracted from different kinds of modal identification methods, i.e., the covariance-driven stochastic subspace identification (SSI-COV) method and the Complexity

Pursuit (CP) algorithm respectively.

Acknowledgements

The project is jointly supported by the National Natural Science Foundation of China with grant numbers 51678278 and 51278226 respectively.

References

- Au, S.K. and Zhang, F.L. (2012), "Fast Bayesian ambient modal identification incorporating multiple setups", *J. Eng. Mech.*, **138**(7), 800-815.
- Au, S.K. and Zhang, F.L. (2016), "Fundamental two-stage formulation for Bayesian system identification, Part I: General theory", *Mech. Syst. Signal Pr.*, **66-67**, 31-42.
- Baghmisheh, M.T.V., Peimani, M., Sadeghi, M.H., Etefagh, M.M. and Tabrizi, A.F. (2012), "A hybrid particle swarm-Nelder-Mead optimization method for crack detection in cantilever beams", *Appl. Soft Comput.*, **12**(8), 2217-2226.
- Beck, J.L., Au, S.K. and Vanik, M.W. (1999), "Bayesian probabilistic approach to structural health monitoring", *J. Eng. Mech.*, **126**(7), 738-745.
- Beck, J.L., Au, S.K. and Vanik, M.W. (2002), "Monitoring structural health using a probabilistic measure", *Comput. Aid. Civil Inf.*, **16**(1), 1-11.
- Begambre, O. and Laier, J.E. (2009), "A hybrid particle swarm optimization - simplex algorithm (PSOS) for structural damage identification", *Adv. Eng. Softw.*, **40**(9), 883-891.
- Chen, B. and Xu, Y.L. (2007), "A new damage index for detecting sudden change of structural stiffness", *Struct. Eng. Mech.*, **26**(26), 315-341.
- Chen, Z.P. and Yu, L. (2015), "An improved PSO-NM algorithm for structural damage detection", *International Conference on Swarm Intelligence*, Beijing, China, June.
- Cheung, S.H. and Beck, J.L. (2009), "Bayesian model updating using hybrid monte carlo simulation with application to structural dynamic models with many uncertain parameters", *J. Eng. Mech.*, **135**(4), 243-255.
- Ching, J. and Beck, J.L. (2004), "Bayesian analysis of the phase II IASC-ASCE structural health monitoring experimental benchmark data", *J. Eng. Mech.*, **130**(10), 1233-1244.
- Farrar, C.R. and Worden, K. (2007), "An introduction to structural health monitoring", *Philos. Tran. A*, **365**(1851), 1-17.
- Friswell, M.I. (2008), "Damage identification using inverse methods", *Philos. Tran. A*, **365**(1851), 393-410.
- Gerist, S. and Maheri, M.R. (2016), "Multi-stage approach for structural damage detection problem using basis pursuit and particle swarm optimization", *J. Sound. Vib.*, **384**, 210-226.
- Jensen, H.A., Esse, C., Araya, V. and Papadimitriou, C. (2017), "Implementation of an adaptive meta-model for Bayesian finite element model updating in time domain", *Reliab. Eng. Syst. Saf.*, 160, 174-190.
- Johnson, E.A., Lam, H.F., Katafygiotis, L.S. and Beck, J.L. (2004), "Phase I IASC-ASCE structural health monitoring benchmark problem using simulated data", *J. Eng. Mech.*, **130**(1), 3-15.
- Katafygiotis, L.S. and Yuen, K.V. (2001), "Bayesian spectral density approach for modal updating using ambient data", *Earthq. Eng. Struct. D.*, **30**(8), 1103-1123.
- Li, Y.Y. and Chen, Y. (2013), "A review on recent development of vibration-based structural robust damage detection", *Struct. Eng. Mech.*, **45**(2), 159-168.
- Pan, C.D., Yu, L., Chen, Z.P., Luo, W.F. and Liu, H.L. (2016), "A hybrid self-adaptive Firefly-Nelder-Mead algorithm for structural damage detection", *Smart Struct. Syst.*, **17**(6), 957-980.
- Pandey, A.K. and Biswas, M. (1994), "Damage detection in structures using changes in flexibility", *J. Sound. Vib.*, **169**(1), 3-17.
- Pandey, A.K., Biswas, M. and Samman, M.M. (1991), "Damage detection from changes in curvature mode shapes", *J. Sound. Vib.*, **145**(2), 321-332.
- Peeters, B. and Roeck, G.D. (2001), "Stochastic system identification for operational modal analysis: a review", *J. Dyn. Syst.-T. Asme*, **123**(4), 659-667.
- Seyedpoor, S.M. (2012), "A two stage method for structural damage detection using a modal strain energy based index and particle swarm optimization", *Int. J. Nonlin. Mech.*, **47**(1), 1-8.
- Shi, Z.Y., Law, S.S. and Zhang, L.M. (2000), "Structural damage detection from modal strain energy change", *J. Eng. Mech.*, **126**(12), 1216-1223.
- Simoen, E., De Roeck, G. and Lombaert, G. (2015), "Dealing with uncertainty in model updating for damage assessment: A review", *Mech. Syst. Signal Pr.*, **56-57**, 123-149.
- Stone, J.V. (2001), "Blind source separation using temporal predictability", *Neural Comput.*, **13**(7), 1559-1574.
- Teughels, A. and De Roeck, G. (2005), "Damage detection and parameter identification by finite element model updating", *Arch. Comput. Meth. E.*, **12**(2), 123-164.
- Xu, H.J., Ding, Z.H., Lu, Z.R. and Liu, J.K. (2015), "Structural damage detection based on Chaotic Artificial Bee Colony algorithm", *Struct. Eng. Mech.*, **55**(6), 1223-1239.
- Yan, Y.J., Cheng, L., Wu, Z.Y. and Yam, L.H. (2007), "Development in vibration-based structural damage detection technique", *Mech. Syst. Signal Pr.*, **21**(5), 2198-2211.
- Yang, Y., Li, S., Nagarajaiah, S., Li, H. and Zhou, P. (2015), "Real-time output-only identification of time-varying cable tension from accelerations via complexity pursuit", *J. Struct. Eng.*, **142**(1).
- Yang, Y. and Nagarajaiah, S. (2013), "Blind modal identification of output-only structures in time-domain based on complexity pursuit", *Earthq. Eng. Struct. D.*, **42**(13), 1885-1905.
- Yu, L. and Li, C. (2014), "A global artificial fish swarm algorithm for structural damage detection", *Adv. Struct. Eng.*, **17**(3), 331-346.
- Yu, L. and Lin, J.C. (2017), "Cloud computing-based time series analysis for structural damage detection", *J. Eng. Mech.*, **143**(1), C4015002.
- Yu, L. and Xu, P. (2011), "Structural health monitoring based on continuous ACO method", *Microelectron. Reliab.*, **51**(2), 270-278.
- Yu, L. and Zhu, J.H. (2015), "Nonlinear damage detection using higher statistical moments of structural responses", *Struct. Eng. Mech.*, **54**(2), 221-237.
- Yuen, K.V., Au, S.K. and Beck, J.L. (2004), "Two-stage structural health monitoring approach for phase I Benchmark studies", *J. Eng. Mech.*, **130**(1), 16-33.
- Yuen, K.V. and Katafygiotis, L.S. (2001), "Bayesian time-domain approach for modal updating using ambient data", *Probabilist. Eng. Mech.*, **16**(3), 219-231.
- Yuen, K.V. and Katafygiotis, L.S. (2003), "Bayesian fast fourier transform approach for modal updating using ambient data", *Adv. Struct. Eng.*, **6**(2), 81-95.
- Yuen, K.V. and Kuok, S.C. (2001), "Bayesian methods for updating dynamic models", *Appl. Mech. Rev.*, **64**(1), Article number 010802.
- Zhang, F.L. and Au, S.K. (2016), "Fundamental two-stage formulation for Bayesian system identification, Part II: Application to ambient vibration data", *Mech. Syst. Signal Pr.*, **66-67**, 43-61.

- Zhang, F.L., Ni, Y.C., Au, S.K. and Lam, H.F. (2015), "Fast bayesian approach for modal identification using free vibration data, Part I - Most probable value", *Mech. Syst. Signal Pr.*, **70-71**, 209-220.
- Zhang, F.L., Xiong, H.B., Shi, W.X. and Ou, X. (2016), "Structural health monitoring of Shanghai Tower during different stages using a Bayesian approach", *Struct. Control Hlth.*, **23**, 1366-1384.